ISSN 0742-0463, Journal of Volcanology and Seismology, 2017, Vol. 11, No. 6, pp. 434–446. © Pleiades Publishing, Ltd., 2017.
Original Russian Text © S.I. Sherman, M.V. Rodkin, E.A. Gorbunova, 2017, published in Vulkanologiya i Seismologiya, 2017, No. 6, pp. 49–63.

A Tectonophysical Analysis of Earthquake Frequency–Size Relationship Types for Catastrophic Earthquakes in Central Asia

S. I. Sherman[a, †], M. V. Rodkin[b, c, *], and E. A. Gorbunova[a]

[a] *Institute of the Earth's Crust, Siberian Branch, Russian Academy of Sciences, ul. Lermontova, 128, Irkutsk, 664033 Russia*

[b] *Institute of Earthquake Prediction Theory and Mathematical Geophysics, Russian Academy of Sciences, Profsozyuznaya ul., 84/32, Moscow, 117485 Russia*

[c] *Institute of Marine Geology and Geophysics, Far East Branch, Russian Academy of Sciences, ul. Nauki, 1B, Yuzhno-Sakhalinsk, 693022 Russia*

**e-mail: rodkin@mitp.ru*

Received March 14, 2017

Abstract—We performed a tectonophysical analysis of earthquake frequency–size relationship types for large Central Asian earthquakes in the regions of dynamical influence due to major earthquake-generating faults based on data for the last 100 years. We identified four types of frequency–size curves, depending on the presence/absence of characteristic earthquakes and the presence or absence of a downward bend in the tail of the curve. This classification by the shape of the tail in frequency–size relationships correlates well with the values of the maximum observed magnitude. Thus, faults of the first type (there are characteristic earthquakes, but no downward bend) with $M_{max} \geq 8.0$ are classified as posing the highest seismic hazard; faults with characteristic earthquakes and a bend, and with $M_{max} = 7.5–7.9$, are treated as rather hazardous; faults of the third type with $M_{max} = 7.1–7.5$ are treated as posing potential hazard; and lastly, faults with a bend, without characteristic earthquakes, and with a typical magnitude $M_{max} \leq 7.0$, are classified as involving little hazard. The tail types in frequency–size curves are interpreted using the model of a nonlinear multiplicative cascade. The model can be used to treat different tail types as corresponding to the occurrence/nonoccurrence of nonlinear positive and negative feedback in earthquake rupture zones, with this feedback being responsible for the occurrence of earthquakes with different magnitudes. This interpretation and clustering of earthquake-generating faults by the behavior the tail of the relevant frequency–size plot shows raises the question about the physical mechanisms that underlie this behavior. We think that the occurrence of great earthquakes is related to a decrease in effective strength (viscosity) in the interblock space of faults at a scale appropriate to the rupture zone size.

DOI: 10.1134/S0742046317060057

1. INTRODUCTION

Central Asia is a unique region on this planet. The great intraplate earthquakes that have occurred there during the last century form a well-pronounced space–time cluster in the Earth's continental lithosphere (Fig. 1), hence the special interest in the statistics and physics of such earthquakes and in the assessment of the hazard they pose. Ordinary statistical approaches to the study of such seismic disasters are not quite effective in view of a comparative rarity of such events. However, the setbacks in long-term prediction (assessment of seismic hazard) for such disastrous earthquakes are due, not only to their rarity, but also to the insufficient understanding of how they occur.

In seismology great earthquakes are classified as those with magnitudes 7 or greater. Our understanding of the physics and mechanisms of large earthquakes (Kostrov, 1975; Sadovskii et al., 1987; Sobolev, 1993; Sobolev and Ponomarev, 2003; Rodkin, 2011) is largely based on analogies with more frequent, hence better known, moderate-magnitude earthquakes. This approach is supported by the fact that the Gutenberg–Richter frequency–magnitude relation, which describes the relationship between the number of events $\log N$ and their magnitudes M, is a straight line in a log–log scale. This tells us that the relationship between the number of earthquakes and their size is constant, that is, shows that earthquakes are self-similar. The self-similarity is not exact, however. The bend at the leftmost termination of the frequency–size plot could be explained by incomplete reporting of smaller events. The frequent departures from the Gutenberg–Richter law at its rightmost end are more interesting. These cannot be explained by mere statistical errors that originate from the rarity of large earth-

† Deceased.

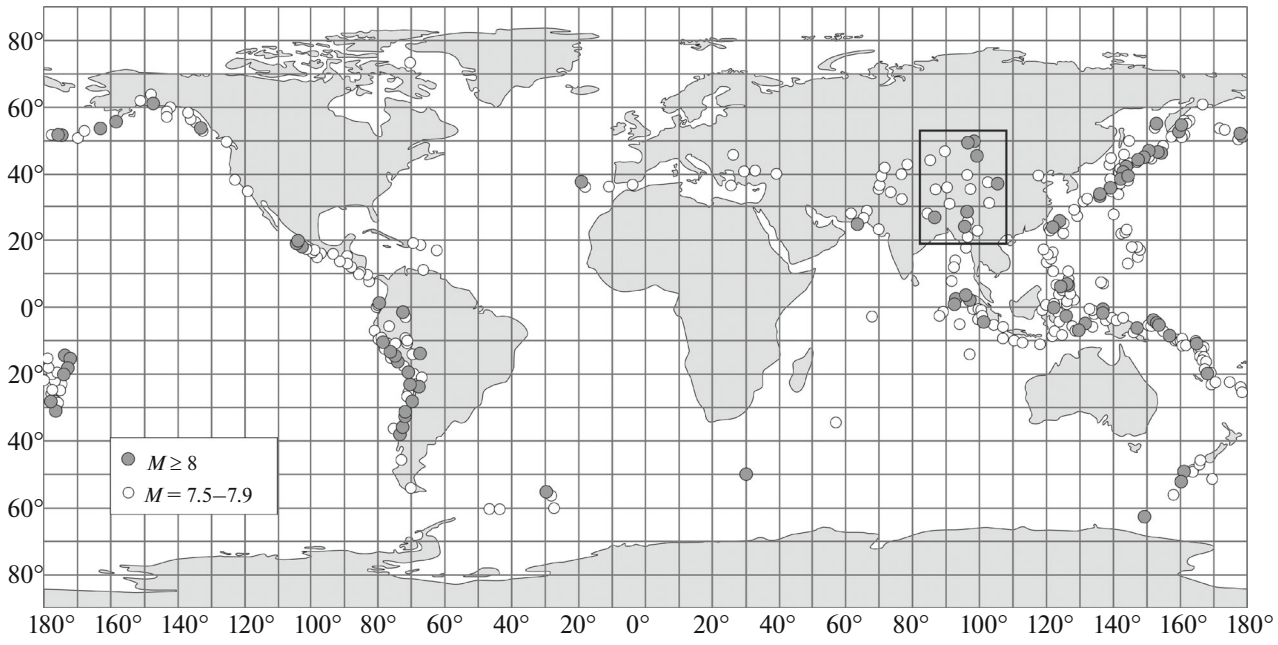

Fig. 1. The cluster of large earthquakes in the Earth's continental lithosphere for the 1800–2015 period. The rectangle encloses the area of catastrophic earthquakes ($M \geq 8.0$).

quakes and incomplete reporting; they also possess a physical meaning.

The departure of the actually observed frequency–size relationship for rare great earthquakes from the classical Gutenberg–Richter law follows from the argument set forth below. The typical values of the parameters that the frequency–size relationship involves and the relationship that connects magnitude and seismic energy for earthquakes are such that, given an increase in magnitude of one, the corresponding earthquake energy increases by a factor of 30, while the rate of events decreases by approximately ten times. When we consider the case of very great events, the relationship is different, with the energy being increased by factors of 14–15 rather than 30 (Kocharyan, 2016), but the situation persists when considered in qualitative terms, viz., events with magnitude ($M + 1$) release more energy than those with magnitude M. The consequence is that seismic energy can go to infinity, which is obviously impossible. It follows that the frequency–size relationship for rare, very great, earthquakes must deviate from the classical Gutenberg–Richter law, ensuring that seismic energy should be bounded over a long time interval, so that the curve must involve a sufficiently steep downward bend in the region of rare very great events.

This paper presents a tectonophysical analysis of the behavior shown by the tails of frequency–size curves for Central Asian earthquakes; we discuss possible reasons why the curves of the different types can occur.

1. THE STATE OF THE PROBLEM

Large earthquakes in Central Asia have always attracted the attention of researchers (Kasahara, 1981; Vikulin and Ivanchin, 2013; Gatinskii et al., 2011; Kocharyan and Spivak, 2003; Rebetskii, 2007; Seminskii, 2001; Stepashko, 2011; Levin and Sasorova, 2012; Sherman, 2013; Koulakov, 2011; Wang and Zhang, 2005; Allen, 1969, among many others). Rare very great earthquakes when plotted in the frequency–size curve are, as should be expected, a source of strong instability in the behavior of the rightmost end of the curve. However, in addition to that effect, one also observes some patterns in the deviations of the tail from the classical Gutenberg–Richter law. A large number of papers have been published that discuss such deviations (Purcaru, 1975; Schwartz and Coppersmith, 1984; Wesnousky et al., 1984; Riznichenko, 1985; Davison and Scholz, 1985; Zhalkovskii, 1988; Pacheco et al., 1992; Vostrikov, 1994; Stirling et al., 1996; Shi-Jun Chen, 1998; Ulomov and Shumilina, 1999; Pisarenko and Rodkin, 2007; Rodkin et al., 2014; Qinghua Han et al., 2015, among many others). The changes in the slope of the frequency–size curve are due to statistically significant departures from the seismicity behavior, as described by the classical Gutenberg–Richter law (Gutenberg and Richter, 1944):

$$\log N = a - bM, \quad (1)$$

where a is the logarithm of the rate of events N at a specified $M = 0$, while b specifies a uniform variation in the rate of events with varying magnitude.

One of the first studies and generalizations of the departures in empirical frequency–size curves from (1) was by Purcaru (1975), who listed nine frequent types of behavior in the tail without trying to analyze the causes of this behavior. Later, researchers tried to introduce additional parameters into the Gutenberg–Richter law, including exponential factors and varying coefficients (Latousakis and Drakopoulos, 1987; Vostrikov, 1994; Kagan, 1994; Laherrere and Sornette, 1998; Shi-Jun Chen et al., 1998) in order to obtain the expected bend at large magnitudes. The most popular option was to divide the frequency–size curve into two parts, with each being described by an equation like (1) with its own slope (see, e.g., Lukk, 1971; Riznichenko, 1985; Davison and Scholz, 1985; Sinadinovski and McCue, 2001). Some other options for tail shape in frequency–size curves continue to be discussed. As an example, Pisarenko and Rodkin (2007, 2010, 2014) discuss numerous examples to show that a gradual downward bend in the curve is the most typical occurrence; moreover, this leads, not only to bounded seismic energy, but also to a distribution law that is bounded on the right. Pacheco et al., (1992); Papadopoulos et al. (1993); Ulomov and Shumilina (1999) noted that the slope of the frequency–size curves frequently changes in the magnitude range $M =$ 5.5–6.5. A new approach was proposed by Sherman et al. (2003), who noted that, starting from the values $M \geq 5.5$–6.5, nearly all earthquakes are controlled by major fault zones that involve a considerable strike-slip component, which may indicate some distinguishing features in the physics of these earthquakes.

Gorbunova and Sherman (2016) showed that the types of behavior for frequency–size curves in the region of large events are more clearly seen when the plot is based on the earthquakes that have been reported, not for the entire seismic zone under consideration, but for areas affected by the dynamic influence of individual major earthquake-generating faults that possess the same character and magnitude of seismotectonic deformations (Sherman, Bornyakov, and Buddo, 1983). This approach was used for an area of high-magnitude intracontinental seismicity in Central Asia. It is that used in the present study.

2. CENTRAL ASIA – A SPECIAL GEODYNAMIC ZONE – A REGION OF GREAT INTRACONTINENTAL EARTHQUAKES IN THE CONTINENTAL LITHOSPHERE

We subdivide large earthquakes (with magnitudes $M \geq 7$) into two sets: large events proper ($7 \leq M < 8$) and very large or disastrous events ($M \geq 8$) (see Fig. 1). All $M \geq 7$ events in Central Asia that have occurred during the last century took place in areas affected by the dynamic influence of long deep-seated lithospheric faults that mostly strike east–west or northwest (Fig. 2). The locations of the very large earthquakes that have occurred in the area can be considered as having been known for the last 200 years.

The region where large earthquakes of Central Asia form clusters is, roughly, a triangle whose northern vertex is in southern Lake Baikal (approximately 105° E and 52° N), while the southern base is enclosed between the points (~70° E, ~35° N) and (~105° E, ~20° N). The base of the triangle for much of its length runs along a boundary that is convex southwestward and roughly bounds the Himalayas from the south (Zhang Jiasheng, 2013; Gatinskii et al., 2011, among others). This identification of a very active seismic territory in the form of a triangle is valid to a first approximation. A more detailed zoning that incorporates geodynamic criteria and the locations of great earthquakes ($M \geq 8$) also defines the boundaries of earthquake occurrence more accurately. This procedure identifies several geodynamic zones where great earthquakes occurred (Sherman, 2015, see Fig. 2). Such zones have been identified based on a set of their geodynamic characteristics, viz., magnitude and the intensity of shaking, crustal thickness and other features of deep structure, the character of lithospheric stresses, and the vectors of present-day movements as revealed by GPS observations (Sherman et al., 2015).

The area where great ($M \geq 8$) earthquakes occurred during the last century contains Tibet, the Himalayas, the Pamirs, and Tien-Shan (Zhang Peizhen et al., 2003). The entire area considered here is characterized by a successive, from south to north, variation in the geological and geophysical parameters of the lithosphere. As one moves away from the area of the Himalayan thrust (the boundary where the Indian plate exerts forces moving northward), the compressive stresses are gradually replaced with shear stresses and decay toward the southern boundary of the Siberian platform. According to geological data, strike-slip movements occur there under crustal compression and are accompanied by the generation of reverse-oblique fractures (in contrast to the generation of normal-oblique movements under different conditions). The variation involves changes in the shape and dimensions of the block structures, crustal thickness decreasing from over 74 km in Tibet to less than 42 km in Tarima and Jungary, successive variation in regional crustal tectonic stresses from dominant compression in the south to combined strike slip and thrusting, as well as strike-slip fields in the Sayans and in the southern Baikal area in the north. In parallel with the variation in the state of stress we observe variations in the directions and rates of horizontal crustal movements (relative to the Eurasian plate). These movements are the highest in the south and in the middle of the central geodynamic zone; further north they are observed to turn eastward, while when nearer to the eastern nearly north–south boundary of the zone (~105° E) the vectors turn southward (Gao Xianglin, 2013; Gan Weijun and Xiao Genru, 2013). The present-day horizontal movements are recording the flow of crustal

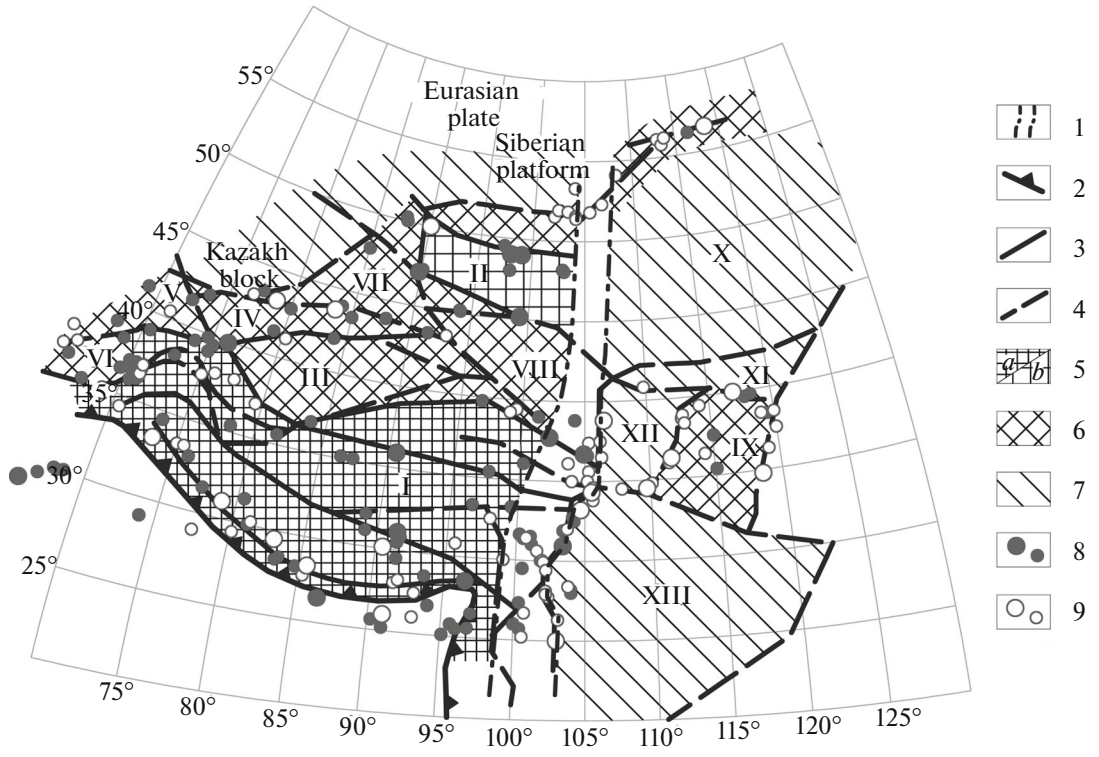

Fig. 2. A map of block structures and active faults in Central Asia that exert control of large modern and historical $M \geq 8$ and $7 \leq M < 8$ earthquakes (based in part on materials from (Zhang, 2013)).

(1) A global trans-regional boundary feature with a transitional structure extending downward to as deep as 600 km (Sherman et al., 2015); (2) Himalayan thrust; (3) active faults whose areas of dynamic influence included $M \geq 8$ seismic events for the past century (1900–2014); (4) active faults whose areas of dynamic influence contain epicenters of $7 \leq M < 8$ events for the past century (1900–2014); (5) active lithosphere blocks (*a* those with a thickened crust (>40 km) and quasi-viscous flow of the material, *b* those with large-amplitude displacements on adjacent faults); (6) active blocks with faults that control $M \geq 7$ seismic events; (7) blocks with sparse dispersed seismicity, and aseismic blocks; (8) epicenters of $M \geq 8$ and $7 \leq M < 8$ (smaller circles) earthquakes that have occurred during the past century (1900–2014); (9) epicenters of $M \geq 8$ and $7 \leq M < 8$ (smaller circles) earthquakes that had occurred during the preceding century (1800–1899). Roman numerals mark the blocks that compose the following geodynamic zones: Central Zone [I Tibet; II Gobi; III Tarima; IV Tien Shan; VII Jungary; VIII Alaxan; Western Zone [V Turanian; VI Tajik]; Eastern Zone [IX East Ordos block (which consists of Taihang, Huaihe, and North China Plain blocks); (X) western part of the Amur block; XI North China block (Yan Shan); XII Ordos block; XIII South China block].

substratum in combination with localized displacements along interblock faults (Burtman, 2012). The flow smooths the boundaries of larger blocks, transforming them into lens-shaped forms that faintly remind one of individual mega-boudines. This localization of deformations and the quasi-flow of rock masses are facilitated by the geodynamic regions that surround the area from the north and west; these regions act like boundaries and arresting barriers, as well as being favored by the nearly triangular shape of the area, so that stress and strain are transmitted to greater distances from the Himalayan Thrust zone.

The northern boundary of this region of intensive intraplate seismicity is the relatively passive Siberian platform with a typical geodynamic platform regime along with the stable Kazakh block. They act as a barrier to the deformation proceeding from the Indian plate. The western boundary of the zone is composed of the area where the Pamirs, Tien Shan, the Turanian and Tadjik blocks converge; that boundary confines the zone of $M \geq 8$ earthquakes from the west. In the east the region is bounded by a transregional, long-evolving, deep-seated structure whose axial line is approximately at 105° E, which is the eastern boundary to the region of large earthquakes in Central Asia during the last century.

Finally, we obtain the result that the area of the cluster of Central Asian earthquakes is different from the surrounding areas in having a more intense lithospheric compression, a thicker crust, a peculiar lens-shaped form of the large blocks that compose the region, considerable present-day displacements along block boundaries, and a more intensive flow of material on an average. If the region had not been confined by the Siberian platform block and by the eastern boundary structure along 105° E, there would have been no concentration of the pressure due to India as far as Lake Baikal. We now proceed to consider seismicity patterns in the areas affected by the dynamic

influence of faults in the cluster of large Central Asian earthquakes.

4. THE ANALYSIS OF THE DATA

4.1. On the Method Used to Construct Earthquake Frequency–Size Relationships

The large Central Asian earthquakes are confined to major faults in the lithosphere. We tried to study patterns in the occurrence of such earthquakes by passing from the analysis of all the seismic zones that compose the cluster to individual major faults and the areas affected by their dynamic influence.

This approach reveals the peculiarities of seismicity in the areas affected by the dynamic influence of individual major faults that control large $M \geq 7.0$ earthquakes.

An area affected by active dynamic influence is understood as the rock mass that surrounds the fault; in this rock mass one observes residual (plastic or discontinuous) and elastic deformations related to fault displacements (Sherman et al., 1983). This is also an area of large deformation due to the earthquakes that occur on the fault. According to Sherman et al. (1983), the width of the area of influence M_{infl} is defined as

$$M_{infl} = bL, \quad (2)$$

where L is fault length (km) and b is a constant of proportionality that is a function of L and varies between 0.03 and 0.09 in the range between transregional to local faults (Sherman et al., 1983). In this paper we assume the width of the zone of influence to be fixed, 50 km, on both sides of the axial fault line, which simplifies the argument and does not contradict the subregional character of most faults under consideration. We consider a set of deep-seated interblock faults in Central Asia (see Fig. 2) that control all $M \geq 7.0$ earthquakes that have occurred during the historical and instrumental periods of observation. We used the cumulative method for constructing frequency–size curves as being more stable and less dependent on the interval of magnitude division (Gorbunova and Sherman, 2016). The method is to plot the magnitudes of the earthquakes that have occurred in the area affected by this fault along the horizontal axis; the vertical axis shows the logarithm of earthquake rate with magnitudes equal to or greater than the magnitude of the earthquake in question. The analysis of the frequency–size curves was carried out by distinguishing sets of points $\{\log N(M_n), M_n\}$ on the curves with different well-pronounced values of the slope in the frequency–size curve. The slope values that are different from the Gutenberg–Richter relation for moderate earthquakes and that lie in the region of large magnitudes characterize the behavior of the tail.

Sherman et al. (2015) showed that the return period of large earthquakes for the entire region of Central Asia under consideration is approximately 25 years. When one considers individual discontinuous structures, one finds that large events are much rarer in the areas affected by their dynamic influence: approximately once every 100 or more years. For this reason, the passage from the consideration of all events to the consideration of zones of influence due to individual faults is an improvement in identifying the peculiarities of seismicity behavior on individual faults, but there is a loss in the quantity of data and in the stability of the result. We now consider tail shapes for individual earthquake-generating faults that have been responsible for large Central Asian earthquakes during the last century in the sense that they can be used to assess the earthquake hazard and for long-term prediction of great earthquakes.

4.2. The Tail Types in Earthquake Frequency–Size Curves in Areas Affected by the Dynamic Influence of the Faults that Control the Cluster of Large and Disastrous Earthquakes in Central Asia

We used our method for each fault under consideration in Central Asia (see Fig. 2) based on the events that have been recorded in the area of its dynamic influence to plot cumulative frequency–size curves. The area of dynamic influence of a fault was assumed to be 50 km wide on both sides of the fault line. The analysis used earthquakes from the NEIC catalog (*National Earthquake ...,* 2016) with magnitudes $M \geq 4$ for the 1900–2014 period. The restriction $M \geq 4$ provides information that, although incomplete, is acceptable for a qualitative analysis of curve shapes. Each curve for earthquakes that have occurred in the area affected by its dynamic influence was estimated from the shape and slope of the tail. The analysis of all 37 faults resulted in the classification of 29 fault zones into four characteristic tail types. Figure 3 shows examples of faults of these four types. The classification of the remaining eight faults (which have not generated any $M \geq 7.5$ earthquakes for the last century) is impeded by lack of data. The 29 faults that are amenable to classification with their identification numbers are shown in Fig. 4. Below, we describe the types of curve identified here; we then interpret them in the framework of the multiplicative cascade model and conclude with a discussion of the physical mechanisms that can lead to such differences in the shape of the tails.

4.3. The Types of Frequency–Size Curves and Fault Classification with Regard to Maximum Possible Magnitudes

We describe the morphology of these tail types in frequency–size curves and classify the respective faults and the areas of their dynamic influence regarding their potential seismic hazard. The first type (see Fig. 3a) exhibits a characteristically decreasing slope in the right part of the curve compared with the bulk of

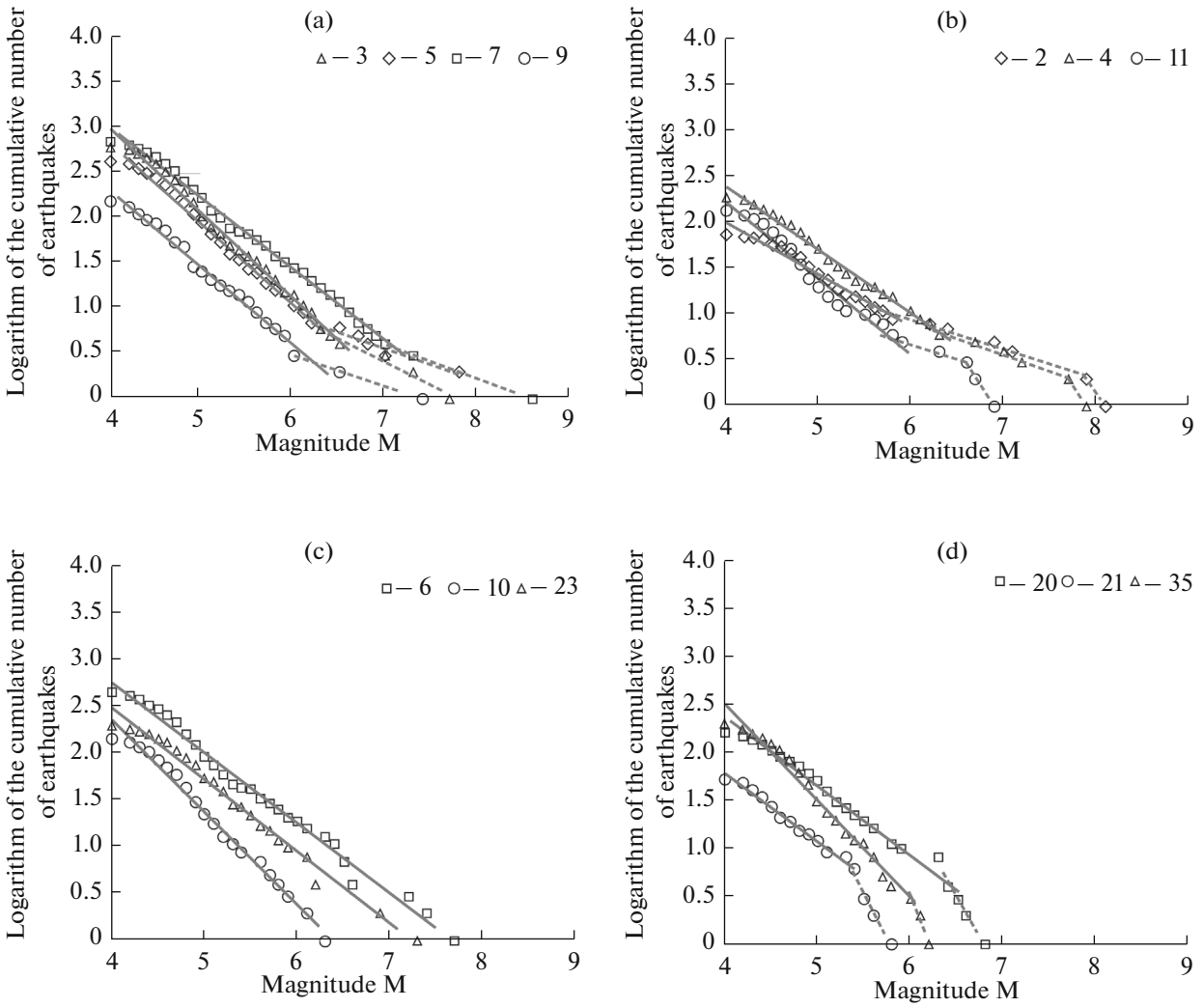

Fig. 3. The types of frequency–size curve classified according to the behavior of the rightmost ends for earthquake-generating faults in Central Asia.

(1–4) types of earthquake frequency–size curve. Numerals at the curves indicate the identification numbers of the faults that are numbered in Fig. 4.

the plot. The slope usually varies in the range of magnitude $M = 6.3 \pm 0.6$. The most characteristic earthquakes for the fault zones with the first type of curve are those with $M \geq 8.0$ (Table 1). Taking the shape of tails into account, we conclude that the size and frequency of such events are substantially above those to be expected from the Gutenberg–Richter relation based on smaller events. The return of similar-sized ($M \geq 8.0$) seismic events for the next 100 years is very likely; this suggests the inference that the faults whose frequency–size curves are of the first type pose the highest seismic hazard (see Fig. 4).

The curves of the second type (see Fig. 3b), as well as those of the first type, show a flattening, but this flattening usually occurs at slightly lower magnitudes $M = 5.7 \pm 0.3$. The tail in a curve of the second type at larger magnitudes ($M = 7.3 \pm 0.5$) develops another bend, with a low angle of slope being replaced with a higher one. However, the maximum magnitudes of seismic events remain high ($M_{max} = 7.1–7.9$), so that the return of an event this size is also quite expectable for the next 100 years. The faults that have curves of the second type can be considered to pose a high potential seismic hazard, but the degree of hazard is somewhat lower compared with the fault zones of the first type (see Fig. 4).

The curves of the third type are based on events with magnitudes reaching $M = 7.1–7.5$, and the slope of the curve is nearly constant throughout the entire range of magnitude (see Fig. 3c). Faults of the third type occur in Central Asia less frequently compared with those of the other types (see Table 1). Since the slope is constant, such faults can also be considered as posing earthquake hazard.

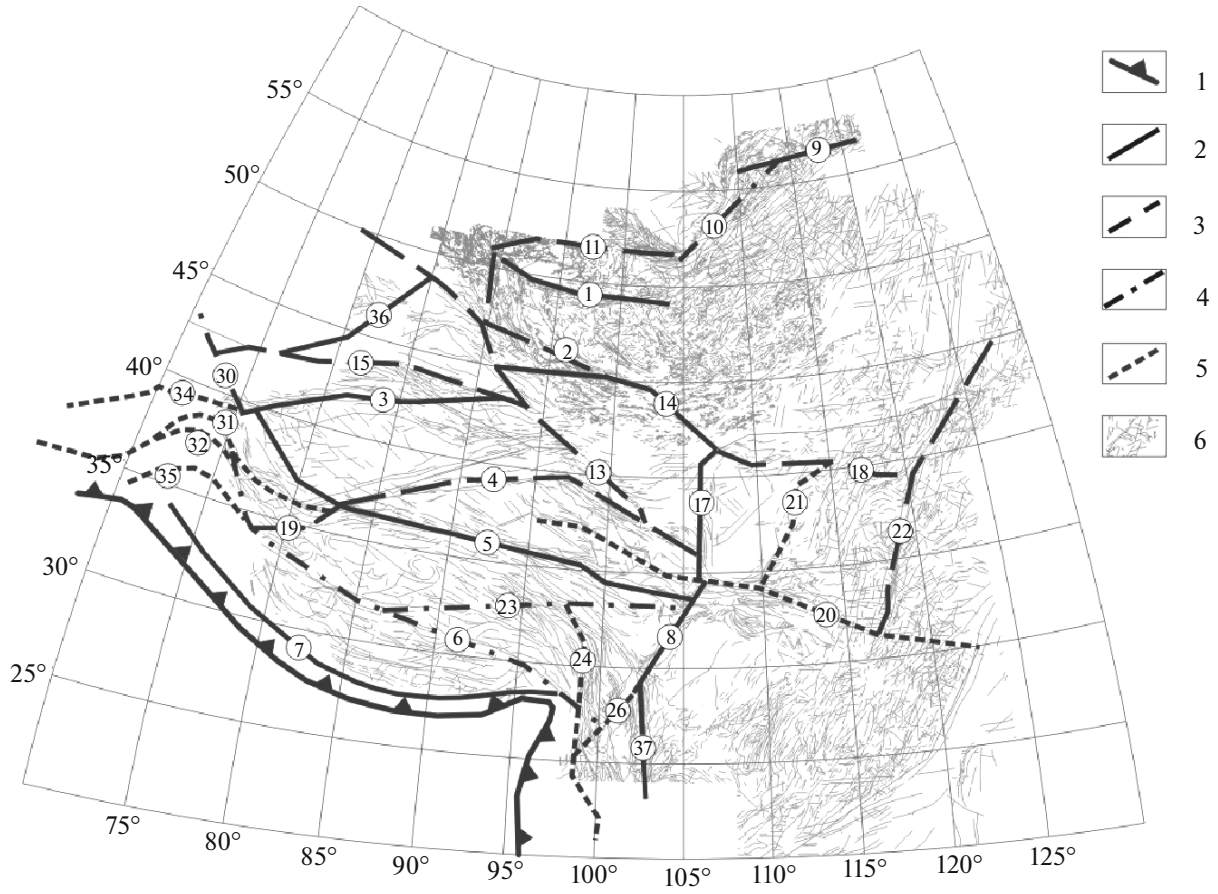

Fig. 4. A map of relative seismic hazard for faults in Central Asia
(1) Southern thrust boundary of the Himalayan seismic belt; (2–5) the degree of seismic hazard of faults: (2) catastrophic, (3) rather high hazard; (4) high hazard, (5) low hazard; (6) other faults. Numerals indicate the fault identification numbers as in Fig. 3.

For the curves of the fourth type (see Fig. 3d), the tail experiences one downward bend in the magnitude range $M = 6.1 \pm 0.6$. The lower magnitudes of recorded earthquakes compared with the faults in the first and second sets, and the downward bend in the curves, all combine to suggest that the fourth type of curve occurs at the least hazardous faults, and the generation of large events with $M > 7.5$ is little likely for the next 100 years.

The above-mentioned tail types are observed systematically for different faults, thus suggesting that certain patterns underlie these types rather than the

Table 1. The main parameters in the types of "tails" in the earthquake frequency–size curves in the areas that are affected by the dynamic influence of earthquake-generating faults in Central Asia for the 1900–2014 period.

Types of "tails" in frequency–size curves of earthquake-generating faults/ number of faults	The number of faults whose areas of dynamic influence have generated earthquakes with the maximum magnitudes				Mean b_1-values in the regression line for the most frequency–size curves	The magnitude value corresponding to the point (points) where the slope of frequency–size curves changes	Mean b_2-values in the regression line for the "tails" of frequency–size curves
	≥ 8.0	7.6–7.9	7.1–7.5	5.7–7.0			
1/9	4	3	1	1	0.82 ± 0.21	6.3 ± 0.6	0.33 ± 0.13
2/9	1	3	3	2	0.77 ± 0.13	5.7 ± 0.3 7.3 ± 0.5	0.34 ± 0.10 1.92 ± 0.84
3/4	–	1	2	1	0.81 ± 0.12	–	–
4/7	–	1	2	4	0.83 ± 0.11	6.1 ± 0.6	2.50 ± 1.57

types being random variations in tail shape due to the occurrence of fewer larger earthquakes. It seems possible on this basis to propose a local (on the scale of individual fault zones) long-term forecast of seismic hazard for the next 100 years. This kind of prediction attains substantially higher spatial resolution (earthquake hazard assessment) compared with the other methods.

Additional support for the real (non-random) existence of the above behaviors of the tail types consists in a good agreement between these types and the results obtained by simulating the seismic process with a nonlinear multiplicative cascade.

4.4. An Interpretation of Tail Types in Frequency–Size Curves Using a Nonlinear Multiplicative Cascade Model

Our interpretation of the above tail-type behaviors (see Fig. 3) employs a nonlinear multiplicative cascade model, NMCM (Rodkin, 2011; Rodkin et al., 2015). The NMCM treats earthquakes as episodes in the relaxation of statistically identical subsystems in a sufficiently large metastable system. The model is different from the other possible approaches in having greater generality, because the modeling is carried out at the level of describing a set of positive and negative, linear and nonlinear feedback connections without specifying the responsible physical processes. Since the NMCM is so general and simple, one can expect acceptable reliability of the general patterns it can identify.

The main tenets of the original multiplicative cascade model (Rodkin, 2011) can be summarized as follows. Suppose an earthquake has begun to occur and the seismic energy it has released by time t_i is X_i . It can continue to occur with probability p or it can stop with probability $(1 - p)$. In case the process terminates at step i, the energy of that event is taken to equal the value X_i that has been reached at this step. If the seismic process continues, we have a larger earthquake whose size X_{i+1} will be, at the next time t_{i+1}, equal to

$$X_{i+1} = r \times X_i, \qquad (3)$$

where $r > 1$ is a parameter (a random parameter in the general case whose mean is greater than 1). Whether the rupture process will stop at this new stage or the earthquake will be occurring further is determined by the same value of probability p, as at the preceding stage. The seismic regime is understood as the set of values of X resulting from the evolution of each simulated event. The avalanche-like process expressed from (3) will always stop at some stage and the value of energy x reached will characterize the energy of this earthquake. An analogue of earthquake magnitude will be defined as $\log(X)$.

For the first step we set earthquake size equal to X_0 (the actual value of X_0 is immaterial for further argument). In that case, according to (3), the probability for the process to stop at the nth stage, obtaining the value $X = X_0 r^n$, would be $(1 - p)p^n$. Thus, we derive the result that the tail of the distribution function $F(X_n > X)$ is described by the relation $(1 - F(X)) = p^{\log(X)/\log(r)}$ whence

$$\log(-F(X)) = \log(p)/\log(r) \times \log(X), \qquad (4)$$

that is to say, we derived a power law for the tail of the distribution function $(1 - F(X))$, similarly to the ordinary Gutenberg–Richter law (for energy or seismic moment). When the parameters p and r are constant, the output of the procedure (3–4) will be a discrete hierarchical distribution of earthquake size. As the random scatter of p and/or r increases, the stepwise character of the distribution is smoothed and the limit will be a distribution that is quite analogous to the ordinary plot of earthquake recurrence in the $\{\log(X), \log(N)\}$ coordinates.

The slope of the frequency–size curve in log–log coordinates $\{\log(X), \log(N)\}$ is equal to $\beta = \log(1/p)/\log(r)$, where the parameter β has a meaning analogous to the slope or the b-value for the Gutenberg–Richter law (for simulated magnitudes $M = \log(X)$).

It is easy to select such values of the numerical parameters r and p and the initial values of X_0 that one obtains the resulting slope of the frequency–size curve and the simulated magnitudes M close to the typical values for the Gutenberg–Richter law. Thus, fixing the average number N of avalanche-like processes per unit time and some time-dependent variability for r and/or p, we obtain a sequence of main-shock magnitudes $M = \log(X)$ that would be similar to that of earthquake magnitudes (main shocks) in the actually observed seismicity.

Even though this model is so simple, it nevertheless describes a known empirical tendency: the time intervals in the occurrence of large magnitude events are in statistical correspondence with lower slopes of the frequency–size curve (Rodkin, 2011). That means that the model is meaningful, even in its simplest form; this indicates promise for subsequent applications and development.

One can clearly see several steps that would lead to a more complex model. Actually observed earthquakes are not independent, the rate of seismic energy release depends on previous events; in particular, the occurrence of aftershocks is a response to a large displacement in the main shock. The requirement for seismicity to be stationary over long intervals of time gives rise to the necessity of a subsequent compensatory diminution of seismic activity. The introduction of such interactions in the model makes it possible for it to describe low-magnitude foreshock increases, the Omori law for aftershocks, and the tendency toward a quasi-periodic behavior like the seismic cycle (Rodkin, 2011). Such complications are unnecessary in the present discussion, because the behavior of the tail is

controlled by rare great events that are assumed to be statistically independent.

Another issue occurs that is important for the problem at hand, viz., that the linear cascade model (3–4), as well as the ordinary Gutenberg–Richter relation, has, as a formal corollary, the inference that the seismic energy is theoretically infinite. This is naturally impossible. The solution of that problem and further development of the cascade model in order to be able to simulate the characteristic earthquakes is attained by modifying (3) by including nonlinear correction terms in the relation. The simplest option is to expand (3) to the form

$$X_{i+1} = rX_i, + r_1(X_i/A_1)^2 - r_2(X_i/A_2)^3, \quad (5)$$

where all parameters are positive, and $A_2 \gg A_1 \gg 1$. The parameter A_1 specifies the range of size for the events (X) in which characteristic earthquakes can occur, while A_2 specifies the range of events where another change in the slope of the curve occurs and the curve develops a downward bend (which is the issue that leads to seismic energy being bounded). The coefficients r_1 and r_2 adjust the rate of change for the curve in the respective ranges of X.

We note that, when considered in the light of (5), the effect of characteristic earthquakes can be related to the decay of effective friction on the fault, as the displacement reaches a rather large value; this is the mechanism in the occurrence of very large earthquakes that was proposed by Kocharyan (2016).

The above procedure for introducing nonlinear terms is actually a scheme that is often used in physics, when small terms of higher orders need to be included in an equation. When dealing with the moderate earthquake energies X (or magnitudes $M = \log(X)$), the introduction of nonlinear terms in (3) is not needed, but it drastically modifies the shape of the curve in the region of rare events with extremely high X. By varying the nonlinear terms, we can draw an analogy with the resulting variants of the nonlinear multiplicative cascade model NMCM and the four types of behavior for the tail of frequency–size curves obtained above (see Fig. 3).

The curves of the first type (see Fig. 3a) follow the ordinary Gutenberg–Richter law for most of their length, while the tail shows the effect of abnormally large, characteristic, earthquakes. These occur in the segment where the curve flattens out. Curves of the first type can be described by the NMCM as given by (5) with the only modification that the second term on the right corresponds to the observed behavior of a curve of this type, while the third term is added from general considerations to ensure that seismic energy be finite.

The second type of tail in frequency–size curves (see Fig. 3b) corresponds to the variant of a complete nonlinear multiplicative cascade after (Rodkin, 2011). The model that describes it is entirely consistent with expression (5) where all terms on the right correspond to observed features in a curve of this type.

The third type of tail (see Fig. 3c), which preserves the slope of the curve throughout the range of magnitudes, merely satisfies the ordinary Gutenberg–Richter law (1); its behavior can be described by the simple relation (3). The theoretical requirement of finite seismic energy requires the addition of a negative nonlinear (quadratic, say) term, which leads to the relation

$$X_{i+1} = rX_i, - r_1(X_i/A_1)^2 \quad (6)$$

Lastly, the fourth type of tail (see Fig. 3d) corresponds to the simple variant of a downward bend in the tail. Unlike the preceding case (6), the downward bend is also required by empirical data, not only by theoretical considerations concerning bounded seismic energy. We note that, according to results from a description of the seismic process in the framework of a theory of extreme values (Pisarenko and Rodkin, 2007, 2010, 2014), this type of behavior is the most frequent. It occurs in the case in which the kinetic equation does not include the term that is responsible for the appearance of abnormally large characteristic earthquakes.

We conclude our discussion of the applicability of the NMCM to the description of empirically observed types of behavior in the tails of frequency–size curves by adding several important remarks. The first remark concerns the requirement of bounded seismic energy. This requirement leads to the existence of a downward bend in the curve, also in cases (types A and C) in which 100-year observations do not reveal such a bend. Naturally, the hypothesis of a theoretically predicted bend is simply guesswork.

The second remark is that, with the above in mind, the four tail types behavior as identified here correspond with four believable situations in the character of the tail in the earthquake frequency–size curve (Table 2). This can be seen as follows. Depending on the physical conditions on a fault of interest, characteristic earthquakes can or cannot occur. Now, depending on the length of the observational series and the mean rate of seismicity, the length can be sufficient or insufficient to observe a downward bend in the recurrence curve.

Below we discuss the physical mechanisms that can be responsible for the occurrence of different types of recurrence curves.

4. ON THE PHYSICAL INTERPRETATION OF DIFFERENT TYPES OF FREQUENCY–SIZE CURVES

Recurrence curves reflect patterns in the failure of the geophysical medium. The ordinary Gutenberg–Richter curve indicates uniformity in failure over all scales. A flattening in a frequency–size curve indicates especially favorable conditions for failure in the rele-

Table 2. The classification of the tail behavior for the earthquake frequency–size curves

Type of curve	Do characteristic earthquakes occur?	Is a 100-year interval sufficient for reliable identification of a downward bend in frequency–size curves?
1	Yes	No
2	Yes	Yes
3	No	No
4	No	Yes

vant scale range. A downward bend in a curve provides evidence of more difficult failure in the relevant range of scales. If we set apart the final downward bend, the key question consists in the factors that favor large-scale failure in the Central Asian area under discussion. The favorable conditions are indicated both by large and great earthquakes that occur there and by frequent cases of flattening in the curves recorded in the area. We now ask: What are the physical conditions that can favor such easy failure?

The occurrence of earthquakes of larger magnitudes indicates large displacements in the responsible faults. Changes in the character of failure may be related either to changes in the applied stresses or to changes in the effective strength of the geological material. Since the regional stresses are the same, this indicates weakening of strength bonds in the rupture zones (on the appropriate spatial scale). Since the Indian plate shows stable GPS rates of thrusting motion, one is forced to hypothesize an approximate stability in the level of tectonic stresses. Hence, it follows that weakened strength bonds under a long-term load are probably the factor that facilitates the occurrence of especially large earthquakes in the region.

The strength in interblock faults during great earthquakes can decrease due to a number of processes. The ones that are most frequently appealed to include the action of fluids (Kissin, 2013; Rodkin et al., 2014), which drastically diminishes the sliding friction between blocks, resulting in large amplitudes of block displacements and the consequent large magnitudes of the earthquakes (Riznichenko, 1985). Other factors can also play a role: catching by uneven surfaces at the contacts of interacting blocks (Dobrovol'skii, 1991, 2009), trigger mechanisms (Sobolev, 2011; Sherman, 2014), changes in sliding motion (Kocharyan, 2015, 2016), and other factors. In this connection we would like to note that smoother block boundaries are frequent in the region under consideration, as the blocks themselves have the shapes of mega-boudines.

The geophysical medium for the rupture zone of a large earthquake is the interblock zone of suitable length and thickness with the appropriate properties, with those showing the highest contrast being fragmentation and mylonitization of rocks or, by contrast, "welding" of rocks by intrusive bodies. In the general case, the change in the properties of such a medium that is required to account for increased seismicity is a decrease in effective strength (viscosity) of the interblock medium at spatial scales that correspond to the rupture zone size of great earthquakes (or as the displacement reaches a certain amplitude). It can be supposed that a change in the properties of the interblock medium occurs, and the medium can be transformed under certain conditions into a medium with reduced effective viscosity (Mogi, 1966; Sherman et al., 2015). Such changes in the physical properties of rock masses in the rupture zone of an earthquake can lead, under stable tectonic stresses, to the occurrence of higher displacement amplitudes, and thus, to the high magnitudes of catastrophic earthquakes (Sherman, 2016).

Further studies in the behavior of tails will reveal quantitative relationships between parameters of the medium at different scales and can suggest a tectonophysical interpretation of these relationships. In this connection it would be helpful to note a certain uniformity of the typical values of the parameters corresponding to the different types of behavior for the tail of frequency–size curves. The slope of the curve in the region where the ordinary Gutenberg–Richter law applies has turned out to be approximately the same for all four types of behavior, viz., 0.8 ± 0.1. The slopes were also identical in the regions of characteristic earthquakes for the first and second types, viz., 0.3 ± 0.1. The intervals of magnitude where bends ordinarily develop do not seem to be accidental either, tending toward the values 6.0 ± 0.3 and 7.0 ± 0.3. The persistence in these values not only furnishes additional evidence in favor of the non-accidental character of the behavior of the four tail types, but may also bear the signatures of characteristic changes in the physical properties of rupture zones, and in this respect may prove important for understanding the physics of failure at different spatial scales, in particular, those appropriate for the fault sizes of great earthquakes.

4. CONCLUSIONS

Catastrophic intraplate earthquakes in the continental lithosphere of Central Asia are controlled by major faults in the lithosphere. We investigated patterns in the space–time location of large seismic events by constructing cumulative frequency–size curves for the areas affected by the dynamic influence of individual major earthquake-generating faults (Gorbunova and Sherman, 2016). Although the procedure involves a sharp drop in available data, the choice of identically deformable zones and comparison between the shapes of frequency–size curve for different earthquake-generating faults have revealed four characteristic tail types behavior in the curves. This classification was used to divide earthquake-gen-

erating faults into sets by the degree of earthquake hazard they pose, which is primarily the range of the maximum possible earthquake size. This classification of faults based on the distributions of the largest earthquakes provides a potentially useful refinement of the commonly adopted classification of earthquake hazard, where the leading parameters are seismicity rate and the slope of the frequency–size curve in the region of moderate-sized earthquakes.

This paper compares two approaches to the analysis of tail behavior in frequency–size curves. One is based on data concerning the recurrence of large earthquakes in the zones affected by the influence of major faults in Central Asia (Sherman et al., 2015) and the other uses the nonlinear multiplicative cascade model (Rodkin et al., 2015). The first of these approaches demonstrated the diversity of tail behavior for empirical curves in connection with differences in the seismicity behavior of the respective fault zones. The second approach enabled us to interpret the diversity of tail behavior in terms of linear and nonlinear, positive and negative feedback relationships that determine the evolution of the seismic process. The next step in this study consists in interpreting these interrelationships in terms of physical processes.

We proposed the hypothesis that the shape of tails in the earthquake frequency–size curves bears signatures of changes in the physical rock properties in rupture zones, changes that imply the occurrence of characteristic (catastrophic) earthquakes. The hypothesis also provided reasons for discussing how the physics of rupture zones of great earthquakes is related to decreased effective viscosity in the rocks at rupture zones and to the rheologic properties of fault zones at a variety of spatial scales. An understanding of rheologic rock properties at the rupture zones of great earthquakes opens the way to introducing parameters of their effective viscosity and relaxation times. The next stage in the development of space–time prediction for catastrophic earthquakes can be reached by making more specific statements toward more concrete modifications of the above general inference on changes in the effective viscosity of earthquake-generating fault zones at scales appropriate to the rupture zones of great earthquakes.

ACKNOWLEDGMENTS

This work was carried out in compliance with the research plan of the Tectonophysical Laboratory at the Institute of the Earth's Crus, Siberian Branch, Russian Academy of Sciences (IEC SB RAS) and was supported in part by the Russian Foundation for Basic Research, project no. 17-05-00349.

REFERENCES

Allen, C.R., *Active Faulting in Northern Turkey, Div. Geol. Sci., Californ. Inst. Tech.,* 1969, pp. 32–34.

Burtman, V.S., The Late Cenozoic geodynamics of Tibet, Tarima, and Tien Shan, *Geotektonika,* 2012, no. 3, pp. 18–46.

Davison, Jr. F.C. and Scholz, C.H., Frequency-moment distribution of earthquakes in the Aleutian arc: a test of the characteristic earthquake model, *Bulletin of the Seismological Society of America,* 1985, vol. 75, no. 5, pp. 1349–1361.

Dobrovol'skii, I.P., *Teoriya podgotovki tektonicheskogo zemletryaseniya* (A Theory of Precursory Processes Prior to Tectonic Earthquakes), Moscow: IFZ AN SSSR, 1991.

Dobrovol'skii, I.P., *Matematicheskaya teoriya podgotovki i prognoza tektonicheskogo zemletryaseniya* (A Mathematical Theory of the Precursory Period and Prediction of Tectonic Earthquakes), Moscow: Fizmatlit, 2009.

Gan Weijun and Xiao Genru, Present-day crustal motion GPS velocity field of central Asia, in *Atlas of Seismotectonics in Central Asia,* Beijing, 2013, pp. 41–42.

Gao Xianglin, Plate dynamics context of seismotectonics in central Asia, in *Atlas of Seismotectonics in Central Asia,* Beijing, 2013, pp. 29–31.

Gatinskii, Yu.G., Vladova, G.L., Prokhorova, T.V., and Rundkvist, D.V., The geodynamics of Central Asia and the prediction of catastrophic earthquakes, *Prostranstvo i Vremya,* 2011, vol. 3, no. 5, pp. 124–134.

Gorbunova, E.A. and Sherman, S.I., The probability of large ($M \geq 7.5$) earthquakes in the fault zones of Central Asia: A tectonophysical analysis, *Geodinamika i Tektonofizika,* 2016, vol. 7, no. 2, pp. 303–314.

Gutenberg, B. and Richter, C.F., Frequency of earthquakes in California, *Bull. Seismol. Soc. Am.,* 1944, vol. 34, pp. 185–188.

Kagan, Y.Y., Observational evidence for earthquakes as a nonlinear dynamic process, *Physica D: Nonlinear Phenomena,* 1994, vol. 77, no. 1, pp. 160–192.

Kasahara, K., *Earthquake Mechanics,* Cambridge University Press, 1981.

Kissin, I.G., Trigger processes: Methodological aspects, participation of fluids, in *Triggernye effekty v geosistemakh* (Trigger Effects in Geosystems), Moscow: GEOS, 2013, pp. 146–152.

Kocharyan, G.G., *Geomekhanika razlomov* (Geomechanics of Faults), Moscow: GEOS, 2016.

Kocharyan, G.G., Another word on possible prevention of earthquakes, in *Triggernye effekty v geosistemakh* (Trigger Effects in Geosystems), Proc. Third All-Russia seminar conference, IDG RAN, Moscow: GEOS, 2015, pp. 30–39.

Kocharyan, G.G. and Spivak, A.A., *Dinamika deformirovaniya blochnykh massivov gornykh porod* (The Dynamics of Deformation in Blocky Rock Massifs), Moscow: IKTs Akademkniga, 2003.

Kostrov, B.V., *Mekhanika ochaga tektonicheskogo zemletryaseniya* (The Mechanics of the Rupture Zone of a Tectonic Earthquake), Moscow: Nauka, 1975.

Koulakov, I., High-frequency P and S velocity anomalies in the upper mantle beneath Asia from inversion of worldwide travel time data, *Journal of Geophysical Research,* 2011, vol. 116, no. B4, B04301.

Laherrere, J. and Sornette, D., Stretched exponential distributions in nature and economy: "fat-tails" with characteristic scales, *The European Physical Journal B-Condensed Matter and Complex Systems,* 1998, vol. 2, no. 4, pp. 525–539.

Latousakis, J. and Drakopoulos, J.A., Modified formula for frequency-magnitude distribution, *PAGEOPH,* 1987, vol. 125, no. 5, pp. 753–764.

Levin, B.V. and Sasorova, E.V., *Seismichnost' Tikhookeanskogo regiona. Vyyavlenie global'nykh zakonomernostei* (Seismicity of the Pacific Region. Identification of Global Patterns), Moscow: Yanus-L, 2012.

Lukk, A.A., The seismicity of the Pyandzh River basin and nonlinear shapes of the frequency–size curve, in *Eksperimental'naya seismologiya* (Experimental Seismology), Moscow: Nauka, 1971, pp. 297–313.

Mogi, K., Pressure dependence of rock strength and transition from brittle fracture to ductile flow, *Bull. Earth. Res. Inst.,* 1966, vol. 44, pp. 215–232.

National Earthquake Information Center (NEIC), 2016. Available from: http://earthquake.usgs.gov

Pacheco, J.F., Scholz, C.H., and Sykes, L.R., Changes in frequency-size relationship from small to large earthquakes, *Nature,* 1992, vol. 355, pp. 71–73.

Papadopoulos, G.A., Skafida, H.G., and Vassiliou, I.T., Nonlinearity of the magnitude-frequency relation in the Hellenic Arc–Trench System and the characteristic earthquake model, *Journal of Geophysical Research,* 1993, vol. 98, no. B10, pp. 17 737–17 744.

Pisarenko, V.F. and Rodkin, M.V., *Raspredeleniya s tyazhelymi khvostami: prilozheniya k analizu katastrof* (Distributions with Heavy Tails: Applications to the Analysis of Catastrophes), *Vychislitel'naya Seismologiya, 38*, Moscow: GEOS, 2007.

Pisarenko, V. and Rodkin, M., *Heavy-Tailed Distributions in Disaster Analysis. Advances in Natural and Technological Hazards Research,* vol. 30, Dordrecht, Heidelberg, London, N. Y.: Springer, 2010.

Pisarenko, V. and Rodkin, M., *Statistical Analysis of Natural Disasters and Related Losses, Springer Briefs in Earth Sciences,* Dordrecht, Heidelberg, London, N. Y.: Springer, 2014.

Purcaru, G., A new magnitude-frequency relation for earthquakes and a classification of relation types, *Geophys. J. R. astr. Soc.* 1975, vol. 42, pp. 61–79.

Qinghua Han, LichenWang, Jie Xua, Carpinteri, A., and Lacidogna, G., A robust method to estimate the b-value of the magnitude–frequency distribution of earthquakes, *Chaos, Solitons and Fractals,* 2015, vol. 81 pp. 103–110.

Rebetskii, Yu.L., *Tektonicheskie napryazheniya i prochnost' prirodnykh massivov* (Tectonic Stresses and the Strength of Natural Rock Massifs), Moscow: Akademkniga, 2007.

Riznichenko, Yu.V., *Problemy seismologii* (Problems in Seismology), Moscow: Nauka, 1985.

Rodkin, M.V., A model of seismicity as a set of avalanche-like relaxation episodes that occur on the set of metastable states, *Fizika Zemli,* 2011, no. 10, pp. 18–26.

Rodkin, M.V., Pisarenko, V.F., Ngo Thi Ly, and Rukavishnikova, T.A., On possible occurrences of the law governing the distribution of rare great earthquakes, *Geodinamika i Tektonofizika,* 2014, vol. 5, no. 4, pp. 893–904.

Rodkin, M.V., Ngo Thi Ly, and Labuntsova, L.M., Expanding the multiplicative cascade model to describe the recurrence of great earthquakes in application to the seismicity of Southeast Asia, *Geofizicheskie Issledovaniya,* 2015, vol. 16, no. 2, pp. 59–69.

Sadovskii, M.A., Bolkhovitinov, L.G., and Pisarenko, V.F., *Deformirovanie geofizicheskoi sredy i seismicheskii protsess* (Deformation in the Geophysical Medium and the Seismic Process), Moscow: Nauka, 1987.

Schwartz, D.P. and Coppersmith, K.J., Fault behavior and characteristic earthquakes: Examples from the Wasatch and San Andreas fault zones, *Journal of Geophysical Research,* 1984, vol. 89, no. B7, pp. 5681–5698.

Seminskii, K.Zh., Tectonophysical patterns in lithospheric destruction: The Himalayan compression zone, *Tikhookeanskaya Geologiya,* 2001, vol. 20, no. 6, pp. 17–30.

Sherman, S.I., Strain waves as a trigger mechanism for seismic activity in seismic zones of continental lithosphere, *Geodinamika i Tektonofizika,* 2013, vol. 4, no. 2, pp. 83–117.

Sherman, S.I., *Seismicheskii protsess i prognoz zemletryasenii: tektonofizicheskaya kontseptsiya* (The Seismic Process and Earthquake Prediction: A Tectonophysical Concept), Novosibirsk: Akademicheskoe Izdatel'stvo Geo, 2014.

Sherman, S.I., Genetic sources and tectonophysical regularities of divisibility of the lithosphere into blocks of various ranks at different stages of its formation: tectonophysical analysis, *Geodynamics & Tectonophysics,* 2015, vol. 6, no. 3, pp. 387–408.

Sherman, S.I., Tectonophysical criteria for the generation of rupture zones of large earthquakes in the seismic zones of Central Asia, *Geodinamika i Tektonofizika,* 2016, vol. 6, no. 4, pp. 495–512.

Sherman, S.I., Berzhinskii, Yu.A., Pavlenov, V.A., and Aptikaev, F.F., *Regional'nye shkaly seismicheskoi intensivnosti. Opyt sozdaniya shkaly dlya Pribaikal'ya* (Regional Scales of Seismic Intensity: Developing a Scale for the Baikal Region), Novosibirsk: SO RAN, Filial GEO, 2003.

Sherman, S.I., Bornyakov, S.A., and Buddo, V.Yu., *Oblasti dinamicheskogo vliyaniya razlomov (rezul'nany modelirovaniya)* (Areas of Dynamic Influence of Faults: Modeling Results), Novosibirsk: Nauka, SO AN SSSR, 1983.

Sherman, S.I., Ma Jin, and Gorbunova, E.A., Recent strong earthquakes and seismotectonics in Central Asia, *Geodynamics & Tectonophysics,* 2015, vol. 6, no. 4, pp. 409–436.

Shi-Jun Chen, Zhi-Cai Wang, and Jiu-Qing Tao, Nonlinear magnitude frequency relation and two types of seismicity systems, *Acta Seismologica Sinica,* 1998, vol. 11, no. 2, pp. 207–218.

Sinadinovski, C. and McCue, K.F., Recurrence relationships for Australian earthquakes, *AEES 2001 Canberra Conference Proceedings,* 2001, Paper 25.

Sobolev, G.A., *Osnovy prognoza zemletryasenii* (Principles of Earthquake Prediction), Moscow: Nauka, 1993.

Sobolev, G.A., *Kontseptsiya predskazuemosti zemletryasenii na osnove dinamiki seismichnosti pri triggernom vozdeistvii* (The Concept of Earthquake Predictability Based on the Dynamics of Seismicity Excited by Trigger Action), Moscow: IFZ RAN, 2011.

Sobolev, G.A. and Ponomarev, A.V., *Fizika zemletryasenii i predvestniki* (Earthquake Physics and Precursors), Moscow: Nauka, 2003.

Stepashko, A.A., Seismodynamics and a deep source responsible for the North China zone of large earthquakes, *Geodinamika i Tektonofizika,* 2011, vol. 2, no. 4, pp. 341–355.

Stirling, M.W., Wesnousky, S.G., and Shimazaki, K., Fault trace complexity, cumulative slip, and the shape of the magnitude-frequency distribution for strike-slip faults: a global survey, *Geophys. J. Int.,* 1996, vol. 124, pp. 833–868.

Ulomov, V.I. and Shumilina, L.S., *Komplekt kart obshchego seismicheskogo raionirovaniya territorii Rossiiskoi Federatsii – OSR-97. Masshtab 1 : 8000000. Ob"yasnitel'naya zapiska i spisok gorodov i naselennykh punktov, raspolozhennykh v seismoopasnykh raionakh* (A Set of General Seismic Zonation Maps for the Area of the Russian Federation (OSR-97). Scale 1 : 8000000. An Explanatory Note and a List of Cities and Other Population Centers Situated in Earthquake-Prone Regions), Moscow: OIFZ, 1999.

Vikulin, A.V. and Ivanchin, A.G., On the modern concept of a blocky hierarchical structure of the geologic medium and some of its consequences for geosciences, *Fiziko-Tekhnicheskie Problemy Razrabotki Poleznykh Iskopaemykh,* 2013, no. 3, pp. 67–84.

Vostrikov, G.A., *Svyaz' parametrov grafika povtoryaemosti, seismicheskogo techeniya i ochaga zemletryaseniya* (Relationships between Parameters of the Recurrence Curve, Seismic Flow, and Earthquake Rupture Zones), Trudy GIN RAN, 1994, no. 482.

Wang S. and Zhang, Z., Plastic-flow waves (slow waves) and seismic activity in Central-Eastern Asia, *Earthquake Research in China,* 2005, vol. 1, pp. 74–85.

Wesnousky, S.G., Scholz, C.H., Shimazaki, K., and Matsuda, T., Integration of geological and seismological data for the analysis of seismic hazard: a case study of Japan, *Bulletin of the Seismological Society of America,* 1984, vol. 74, no. 2, pp. 687–708.

Zhalkovskii, N.D., Zakon povtoryaemosti zemletryasenii i nekotorye ego sledstviya (The Law of Earthquake Recurrence and Some Consequences from It). Novosibirsk, 1988.

Zhang Jiasheng, Aeromagnetic anomalies in central Asia and their tectonic implication, in *Atlas of Seismotectonics in Central Asia,* Beijing, 2013, pp. 25–26.

Zhang Peizhen, Deng Qidong, Zhang Guomin, et al., Geology of the fault zones, *Science in China,* 2003, vol. 46, pp. 13–24.

Translated by A. Petrosyan